



Diluent modified weakly solvating electrolyte for fast-charging high-voltage lithium metal batteries

Haining Peng^a, Huijun Liu^{a,*}, Chengzong Li^b, Yingfu Li^a, Qizhi Chen^a, Tao Li^{b,*}

^a School of Chemistry and Chemical Engineering, University of South China, Hengyang 421000, China

^b School of Resource Environment and Safety Engineering, University of South China, Hengyang 421000, China

ARTICLE INFO

Article history:

Received 4 January 2024

Accepted 23 January 2024

Available online 1 February 2024

Keywords:

Lithium metal batteries

Weakly solvating electrolyte

Fast-charging

High-voltage

Diluent

ABSTRACT

Weakly solvating electrolyte (WSE) demonstrates superior compatibility with lithium (Li) metal batteries (LMBs). However, its application in fast-charging high-voltage LMBs is challenging. Here, we propose a diluent modified WSE for fast-charging high-voltage LMBs, which is formed by adding diluent of 1,1,2,2-tetrafluoroethyl-2,2,3,3-tetrafluoropropyl ether (TTE) into the tetrahydropyran (THP) based WSE. A relatively loose solvation structure is formed due to the formation of weak hydrogen bond between TTE and THP, which accelerates the de-solvation kinetics of Li⁺. Besides, more anions are involved in solvation structure in the presence of TTE, yielding inorganic-rich interphases with improved stability. Li (30 μm)||LiNi_{0.5}Co_{0.2}Mn_{0.3}O₂ (4.1 mAh/cm²) batteries with the TTE modified WSE retain over 64% capacity retention after 175 cycles under high rate of 3 C and high-voltage of 4.5 V, much better than that with pure THP based WSE. This work points out that the combination of diluent with weakly solvating solvent is a promising approach to develop high performance electrolytes for fast-charging high-voltage LMBs.

© 2024 Published by Elsevier B.V. on behalf of Chinese Chemical Society and Institute of Materia Medica, Chinese Academy of Medical Sciences.

High-voltage lithium metal batteries (LMBs) with energy density over 400 Wh/kg are achievable when pushing all materials and battery parameters to their limits [1,2], for example, elevated charging voltage (>4.3 V) [3], limited Li metal (<30 μm) [4], high loading cathode (>3.5 mAh/cm²) [5], and lean electrolyte (<3 g/Ah) [6]. However, such stringent requirements pose great challenges for electrolyte to maintain a satisfactory cycling life. The commercial carbonate-based electrolyte causes severe Li/electrolyte parasitic reactions and uncontrollable dendritic Li growth, leading to rapid Li consumption and short cycle life of high-voltage LMBs [7,8]. In particular, the parasitic reactions and dendritic Li growth will be further accelerated in the conditions of high-voltage and fast-charging. Thus, designing electrolytes that are compatible with high-voltage LMBs is highly desirable and urgent.

Extensive research has been devoted to electrolyte engineering, including additives-modified electrolytes [9–11], fluorinated electrolytes [12,13], dual-salt electrolytes [14,15], high concentration electrolytes (HCEs) [16–18], localized high concentration electrolytes (LHCEs) [19–22], weakly solvating electrolytes (WSEs) [23–26], *etc.* [27–30]. Among them, HCEs, LHCEs and WSEs stand out as featuring an anion-rich solvation structure, which changes the SEI chemistry and Li⁺ de-solvation kinetics. Specifically, the anion-

dominated solvates generally result in an anion-derived inorganic-rich solid electrolyte interphase (SEI), which is believed to be more efficient in ion-transport and electron-blocking than the solvent-derived organic-rich SEI [31–33]. Moreover, the weak interaction between Li⁺ and weakly solvating solvent in WSEs can facilitate the Li⁺ de-solvation process. However, the practical application of HCEs is hindered by high viscosity, high cost and poor wettability. To circumvent the deficiencies of HCEs, an inert diluent (for example, the most widely used hydrofluoroethers, HFEs) was added to HCEs to prepare LHCEs. Despite the superior physiochemical properties of LHCEs, the introduction of large amount of HFE greatly increases the cost and density of electrolyte (the density of HFEs is generally >1.4 g/cm³) [34]. In WSEs, weakly solvating solvent, such as 1,4-dioxane (1,4-DX) [35], 1,2-diethoxyethane (DEE) [36], diethoxymethane (DEM) [37] and tetrahydropyran (THP) [38], will cause low ionic conductivity because of the insufficient solvation. To simultaneously achieve high Li plating/stripping Coulombic efficiency (CE), sufficient oxidative stability, and high ionic conductivity of WSEs, new weakly solvating solvents with fine-tuned solvation capability have been synthesized [13,39]. Representatively, Bao, Cui, and co-workers reported a series of fluorinated-DEE molecules that endow the electrolytes with balanced properties [40]. Li, Johnson and co-workers reported a sulfonamide-based WSE that enables the stable cycling of Li||NMC811 battery under ultra-high-voltage (4.7 V) [41]. Despite improved electrochemical

* Corresponding authors.

E-mail addresses: liuhuijun@usc.edu.cn (H. Liu), li-tao@usc.edu.cn (T. Li).

performances have been achieved by using these fluorinated weakly solvating solvents, the time/cost-consuming synthetic processes may hinder large-scale applications. Therefore, it is highly desirable to developing commercially available low-cost high-performance WSEs for high-voltage LMBs.

Here, we select a commercially available fluorine-free tetrahydropyran (THP) as weakly solvating solvent and a small amount of diluent (1,1,2,2-tetrafluoroethyl-2,2,3,3-tetrafluoropropyl ether, TTE) as co-solvent to develop a diluent modified WSE for high-voltage LMBs. The weak interaction between TTE and THP lead to the formation of a relatively loose solvation structure, which accelerates the de-solvation kinetics of Li^+ . Besides, more anions are involved in solvation structure in the presence of TTE, yielding inorganic-rich interphases with improved stability. $\text{Li} (30 \mu\text{m}) \parallel \text{LiNi}_{0.5}\text{Co}_{0.2}\text{Mn}_{0.3}\text{O}_2$ (NCM523, 4.1 mAh/cm^2) batteries with the TTE modified WSE retain over 64% capacity retention after 175 cycles under high rate of 3 C and high-voltage of 4.5 V, much better than that with pure THP based WSE. This work provides an economic way to design high-performance WSEs for high-voltage LMBs.

A commercially available fluorine-free cyclic ether (THP) is selected as weakly solvating solvent for the preparation of WSE. Cyclic THP molecular with one O atom demonstrates weaker solvating capability than the widely used linear 1,2-dimethoxyethane (DME) which forming strong chelating structure with Li^+ (Fig. S1 in Supporting information). Two electrolytes were prepared, i.e., 2.0 mol/L LiFSI in DME and 2.0 mol/L LiFSI in THP, denoted as 2M-LiFSI-DME and base WSE, respectively. The two electrolytes were evaluated in $\text{Li} (30 \mu\text{m}) \parallel \text{NCM523} (3.0 \text{ mAh/cm}^2)$ batteries. $\text{Li} \parallel \text{NCM523}$ batteries with base WSE showed a prolonged cycle life of 137 cycles at 92% of initial discharge capacity compared to that of 2M-LiFSI-DME (100 cycles, 78% capacity retention) (Fig. 1a), which should be ascribed to the weakly solvating structure of base WSE. To further improve the cycling performance, a small amount of diluent (TTE) was added into base WSE to prepare the electrolyte of 2.0 mol/L LiFSI in THP/TTE, denoted as diluent modified WSE, in which the ratio of THP/TTE was optimized to be 9:1 (v/v) according to the rate capability (Fig. S2 in Supporting information). As shown in Figs. 1a and b, further enhanced cycling performance and suppressed voltage polarization were achieved in diluent modified WSE with 93% capacity retention after 195 cycles, verifying the beneficial effect of diluent on WSE. Moreover, the improvement in cycling performance is more pronounced under higher cut-off voltage of 4.5 V (the oxidation voltage of diluent modified WSE is higher than 4.5 V, Fig. S3 in Supporting information) and high charge/discharge rate. Compared to base WSE, diluent modified WSE showed significantly higher discharge capacities at 1.5 C and 3 C (Fig. 1c). Then, we further evaluated the long cycling performance at high rate of 3 C (7 mA/cm^2). Strikingly, $\text{Li} \parallel \text{NCM523}$ batteries with diluent modified WSE exhibited a discharge capacity of 2.9 mAh/cm^2 at 3 C and a capacity retention of 64% after 175 cycles, much higher than base WSE (only 1.7 mAh/cm^2 at 3 C, 54% after 175 cycles) (Fig. 1d).

The solvation structure of the above-mentioned electrolytes was investigated by Raman spectroscopy to clarify the mechanism of the performance improvement (Fig. 2a). The free anion (FA) ratio in base WSE (19.6%) is much lower than that in 2M-LiFSI-DME (60.1%) (Fig. 2b), confirming that the solvating power of THP is weaker than DME. With the addition of TTE in base WSE, the peak area ratios assigned to AGG-I (one FSI^- coordinates two Li^+) and AGG-II (one FSI^- coordinates more than two Li^+) increase from 21.9% to 27.1%, 7.4% to 10.5%, respectively (Fig. 2b), indicating that the introduction of diluent can strengthen the interaction between Li^+ and FSI^- . The increased ratio of AGGs in diluent modified WSE induced slightly lower ionic conductivity due to the low diffusion rates of AGGs (Fig. S4 in Supporting information). The enhanced

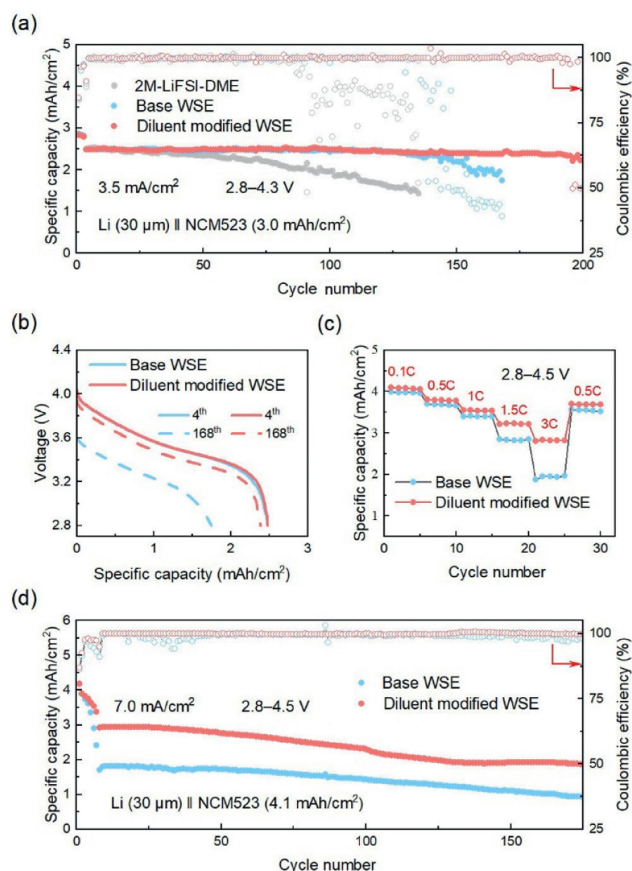


Fig. 1. (a) Cycling performances of $\text{Li} \parallel \text{NCM523}$ batteries in different electrolytes under cut-off voltage of 4.3 V and a current density of 3.5 mA/cm^2 . (b) Corresponding discharge curves of $\text{Li} \parallel \text{NCM523}$ batteries cycled in base WSE and diluent modified WSE. (c) Rate capabilities of $\text{Li} \parallel \text{NCM523}$ batteries in base WSE and diluent modified WSE. (d) Cycling performances of $\text{Li} \parallel \text{NCM523}$ batteries in base WSE and diluent modified WSE under cut-off voltage of 4.5 V and a current density of 7.0 mA/cm^2 .

Li^+ - FSI^- interactions in diluent modified WSE was further confirmed by molecular dynamics (MD) simulations, with representative snapshots shown in Fig. S5 (Supporting information). Radial distribution functions (RDFs) and coordination numbers (CN) were calculated for Li^+ - FSI^- (Fig. 2c) and Li^+ -solvent (Fig. S6 in Supporting information), respectively. 2M-LiFSI-DME displays lower CN of Li^+ - FSI^- (3.195) and higher CN of solvents (2.587). By contrast, in the base WSE, one Li^+ is solvated by 3.947 FSI^- and 0.04 THP solvents on average, confirming the weakly solvating power of THP. Moreover, diluent modified WSE shows the highest CN of Li^+ - FSI^- (3.976) and the lowest CN of solvents (0.022), indicating the further enhanced Li^+ - FSI^- interactions. It is speculated that there exists an interaction between TTE and THP, which further promotes the engagement of FSI^- in the Li^+ solvation structures. To verify this speculation, we performed Fourier transform infrared spectra (FTIR) absorption spectra analysis of THP, TTE, and diluent modified WSE. In the presence of TTE, the absorption peaks around 813 cm^{-1} and 1098 cm^{-1} , assigned to the $-\text{C}-\text{O}-\text{C}-$ symmetric stretching vibration (ν_s) and asymmetric stretching vibration (ν_{as}) of THP respectively, shift to lower frequency (Fig. 2d), which reflects the interaction between TTE and THP. The intermolecular interaction was further verified by ^1H NMR spectra [42–44]. The chemical shifts of H in TTE and THP move to the opposite direction, which is possibly related to the formation of weak hydrogen bond between TTE and THP, with $-\text{CF}_2\text{H}$ group in TTE and O in THP acting as hydrogen bond donor and acceptor, respectively (Fig. 2e) [45,46]. Concretely, the formation of hydrogen bond induces a shielding

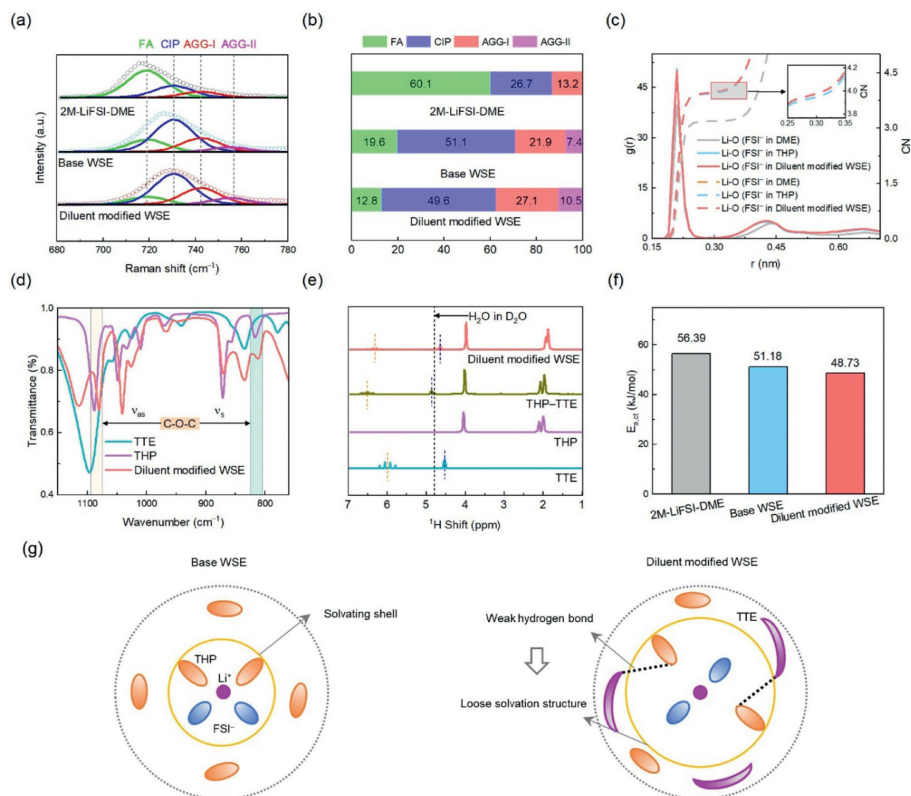


Fig. 2. (a) Raman spectra of the different electrolytes. (b) The ratio of different solution structures in different electrolytes calculated from (a). (c) RDF and CN for Li^+ and FSI^- coordination in different electrolytes. (d) FTIR spectra of pure TTE solvent, THP solvent and diluent modified WSE. (e) ^1H NMR spectra of pure TTE, THP, THP-TTE (9:1, v/v) and diluent modified WSE. (f) An Arrhenius fit was used to determine the de-solvation energy in different electrolytes. (g) Schematics illustrating the effect of hydrogen bond between TTE and THP on the solvation structure diluent modified WSE.

effect on the H in THP and a de-shielding effect on the H in TTE, thus the chemical shift of H in TTE increases while that of H in THP decreases. When adding 2.0 mol/L LiFSI in the mixture of THP and TTE, the chemical shifts of H in TTE decrease slightly, suggesting that the effect of hydrogen bond is slightly weakened by the coordination of THP with Li^+ . In other words, the interaction between TTE and THP is expected to weaken the coordination of THP with Li^+ and result in the formation of a relatively loose solvation structure. As expected, diluent modified WSE demonstrated a much lower Li^+ de-solvation energy (48.73 kJ/mol) than 2M-LiFSI-DME (56.39 kJ/mol) and base WSE (51.18 kJ/mol) (Fig. 2f and Fig. S7 in Supporting information), confirming the formation of a relatively loose solvation structure in diluent modified WSE. Besides, a slightly improved Li^+ transference number was also observed in diluent modified WSE (Fig. S8 in Supporting information). Schematics are provided to demonstrate interaction between TTE and THP and its effect on the solvation structure (Fig. 2g).

The Columbic efficiency (CE) of Li plating/stripping in base WSE and diluent modified WSE was evaluated in Li||Cu batteries. As shown in Fig. 3a, diluent modified WSE shows a higher CE (99.6%) and lower overpotential than that of base WSE (99.4%), suggesting that diluent modified WSE induces more uniform Li deposition and stripping. Scanning electron microscopy (SEM) characterization confirmed that more uniform and larger Li granules were formed in diluent modified WSE (Fig. 3c) than those in base WSE (Fig. 3b). Uniform and larger Li deposition is expected to mitigate the side reactions between electrolyte and Li, thus maintaining a stable Li/electrolyte interface. The interfacial resistance evolution of Li||NCM523 batteries with base WSE and diluent modified WSE was investigated by electrochemical impedance spectroscopy (EIS). The interfacial resistance of Li||NCM523 batteries with base WSE showed a significant increase (39%) from the 8th to 50th cycles, while the value increased by only 9% in the case of diluent

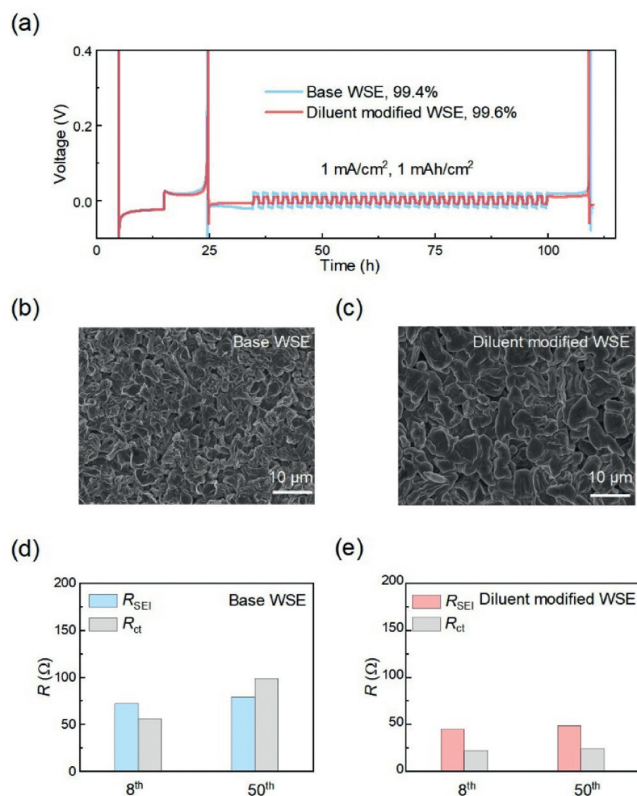


Fig. 3. (a) CE of Li||Cu batteries using different electrolytes. SEM images of the Li deposition morphologies in Cu||NCM523 batteries with (b) base WSE and (c) diluent modified WSE. The evolution of interfacial resistance of Li||NCM523 batteries with (d) base WSE and (e) diluent modified WSE.

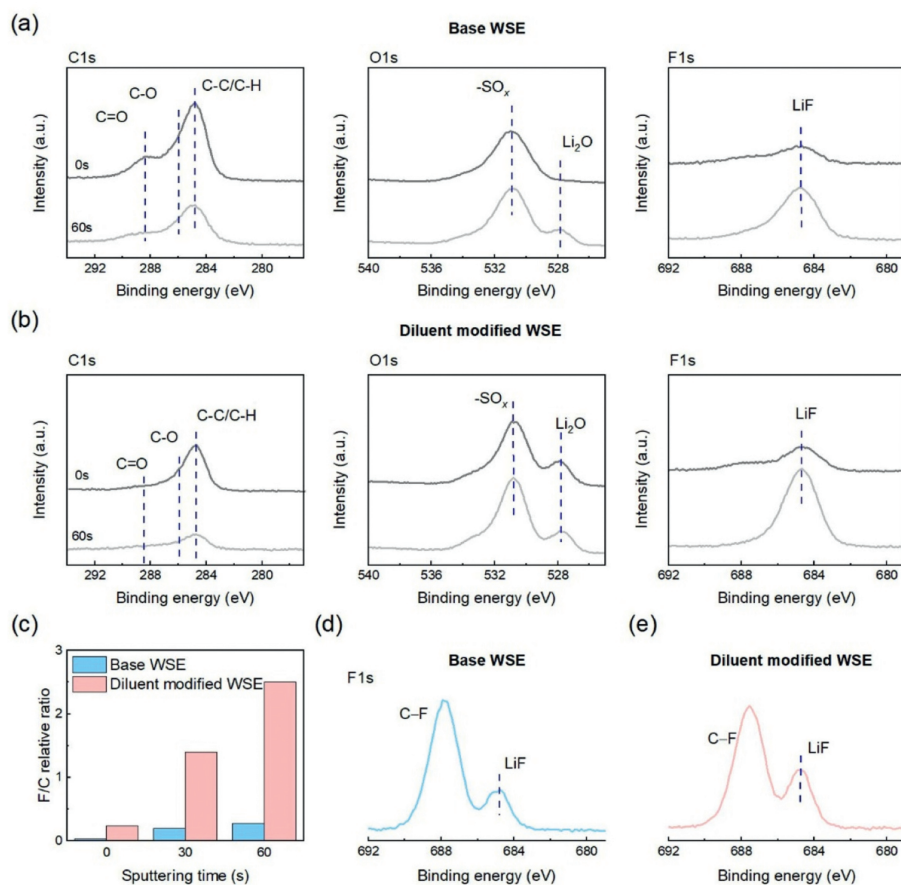


Fig. 4. C 1s, O 1s and F 1s depth profiles of SEI formed in (a) base WSE and (b) diluent modified WSE. Atomic ratios of (c) F/C in SEI samples formed in different electrolytes. F 1s spectra of CEI derived from (d) base WSE and (e) diluent modified WSE.

modified WSE (Figs. 3d and e, Fig. S9 and Table S1 in Supporting information). The results of SEM and EIS indicate that diluent modified WSE enables the formation of an efficient and durable SEI, thus contributing to compact Li deposition and mitigated interfacial resistance increase.

X-ray photoelectron spectroscopy (XPS) characterization was performed to discern the compositional difference of SEI formed in Li||NCM523 batteries with different electrolytes. In both SEI samples formed in base WSE and diluent modified WSE, a strong C-C peak at 284.8 eV assigned to organic components dominated the C 1s spectra, which remarkably decreased upon Ar⁺ etching, indicating that the SEI samples consist of a polymer-rich outer layer and an inorganic inner layer (Figs. 4a and b) [38,47]. From the O 1s, F 1s, S 2p and N 1s spectra of the two SEI samples, the relative intensity of Li₂O, LiF, Li₂S and LiN_x in diluent modified WSE is stronger than those in base WSE, indicating the SEI formed in diluent modified WSE is richer in anion-derived species (Figs. 4a and b, Fig. S10 in Supporting information). Inorganics like Li₂O, LiF, and LiN_x in SEI could efficiently accelerate ion transport and blocks electron tunneling, thus the formation of abundant Li₂O and LiF in the case of diluent modified WSE is responsible for the improved SEI stability. The F/C ratio in SEI samples were further compared, which represent the preference for anion-to-solvent decomposition because F are exclusive to the anions (FSI⁻) while C is exclusive to the solvent (THP). As shown in Fig. 4c, the F/C ratio in SEI sample of diluent modified WSE was significantly higher than that of base WSE, suggesting that more FSI⁻ decomposition occurs in diluent modified WSE. On the cathode side, the CEI derived from diluent modified WSE showed a stronger peak of LiF than that of base WSE (Figs. 4d and e), which is believed

to be beneficial for stabilizing the high-voltage cathode/electrolyte interface [48].

In summary, we propose a diluent modified WSE for fast-charging high-voltage LMBs by introducing a small amount of diluent (TTE) into a THP-based WSE. FTIR and NMR analysis demonstrate that weak hydrogen bond exists between TTE and THP, which accelerates the de-solvation kinetics of Li⁺ by forming a relatively loose solvation structure. Besides, more anions are involved in solvation structure in the presence of TTE, contributing to the formation of an inorganic-rich SEI in diluent modified WSE. Both the loose solvation structure and inorganic-rich SEI enable Li||NCM523 batteries with diluent modified WSE to exhibit enhanced electrochemical performance. Li (30 μm)||NCM523 (4.1 mAh/cm²) batteries with the TTE modified WSE retain over 64% capacity retention after 175 cycles under high rate of 3 C and high-voltage of 4.5V, much better than that with pure THP based WSE. The diluent-weakly solvating solvent interactions approach can inspire future development of high-performance electrolytes for fast-charging high-voltage LMBs.

Declaration of competing interest

The authors declare that they have no known competing financial interests or personal relationships that could have appeared to influence the work reported in this paper.

Acknowledgments

This work was supported by Hengyang City, Hunan Province Science and Technology Innovation Project (No. 202250045319),

the National Natural Science Foundation of China (Nos. 11375084, 21808125), the Scientific Research Planning Project of Jilin Provincial Education Department (No. JJKH20241249KJ). The theoretical calculations were supported by Institute of Theoretical Chemistry, College of Chemistry, Jilin University and Associate Professor Luyi Zou (Jilin University).

Supplementary materials

Supplementary material associated with this article can be found, in the online version, at doi:10.1016/j.ccl.2024.109556.

References

- [1] B. Liu, J.G. Zhang, W. Xu, *Joule* 2 (2018) 833–845.
- [2] Q. Wang, B. Liu, Y. Shen, et al., *Adv. Sci.* 8 (2021) 2101111.
- [3] Y. Zhao, T. Zhou, T. Ashirov, et al., *Nat. Commun.* 13 (2022) 2575.
- [4] J. Lee, S.H. Jeong, J.S. Nam, et al., *EcoMat* 5 (2023) 12416.
- [5] L. Chang, W. Yang, K. Cai, et al., *Mater. Horiz.* 10 (2023) 4776–4826.
- [6] Q. Ran, Z. Song, J. Liu, et al., *ACS Sustain. Chem. Eng.* 11 (2023) 15732–15742.
- [7] Y. Liu, D. Lin, Y. Li, et al., *Nat. Commun.* 9 (2018) 3656.
- [8] X. Zheng, L. Huang, W. Luo, et al., *ACS Energy Lett.* 6 (2021) 2054–2063.
- [9] P. Lai, B. Huang, X. Deng, et al., *Chem. Eng. J.* 461 (2023) 141904.
- [10] Q.K. Zhang, X.Q. Zhang, J. Wan, et al., *Nat. Energy* 8 (2023) 725–735.
- [11] D. Wu, C. Zhu, H. Wang, et al., *Angew. Chem. Int. Ed.* 63 (2023) e202315608.
- [12] X. Fan, X. Ji, L. Chen, et al., *Nat. Energy* 4 (2019) 882–890.
- [13] Z. Yu, H. Wang, X. Kong, et al., *Nat. Energy* 5 (2020) 526–533.
- [14] S. Liu, Q. Zhang, X. Wang, et al., *ACS Appl. Mater. Interfaces* 12 (2020) 33719–33728.
- [15] F. Fu, Y. Zheng, N. Jiang, et al., *Chem. Eng. J.* 450 (2022) 137776.
- [16] J. Wang, Y. Yamada, K. Sodeyama, et al., *Nat. Commun.* 7 (2016) 12032.
- [17] Y. Yamada, J. Wang, S. Ko, et al., *Nat. Energy* 4 (2019) 269–280.
- [18] O. Borodin, J. Self, K.A. Persson, et al., *Joule* 4 (2020) 69–100.
- [19] S. Chen, J. Zheng, L. Yu, et al., *Joule* 2 (2018) 1548–1558.
- [20] C. Zhang, S. Gu, D. Zhang, et al., *Energy Storage Mater.* 52 (2022) 355–364.
- [21] C. Li, Y. Li, Z. Chen, et al., *Chin. Chem. Lett.* 34 (2023) 107852.
- [22] Z. Wang, L.P. Hou, Q.K. Zhang, et al., *Chin. Chem. Lett.* 35 (2024) 108570.
- [23] J. Choi, H. Jeong, J. Jang, et al., *J. Am. Chem. Soc.* 143 (2021) 9169–9176.
- [24] S. Sawayama, R. Ochi, H. Mimura, et al., *J. Phys. Chem. C* 125 (2021) 27098–27105.
- [25] Z. Cao, X. Zheng, M. Zhou, et al., *ACS Energy Lett.* 7 (2022) 3581–3592.
- [26] X. Hu, J. Liu, Y. Yang, et al., *Chin. Chem. Lett.* 34 (2023) 108456.
- [27] W. Wu, Y. Bai, X. Wang, et al., *Chin. Chem. Lett.* 32 (2021) 1309–1315.
- [28] S. Zhang, B. Cheng, Y. Fang, et al., *Chin. Chem. Lett.* 33 (2022) 3951–3954.
- [29] Q. Sun, Z. Cao, Z. Ma, et al., *Adv. Funct. Mater.* 33 (2022) 2210292.
- [30] Y. Zou, G. Liu, Y. Wang, et al., *Adv. Energy Mater.* 13 (2023) 2300443.
- [31] C. Zhu, C. Sun, R. Li, et al., *ACS Energy Lett.* 7 (2022) 1338–1347.
- [32] T.D. Pham, A. Bin Faheem, J. Kim, et al., *Small* 18 (2022) 2107492.
- [33] M.Y. Zhou, X.Q. Ding, J.F. Ding, et al., *Joule* 6 (2022) 2122–2137.
- [34] J. Wu, T. Zhou, B. Zhong, et al., *ACS Appl. Mater. Interfaces* 14 (2022) 27873–27881.
- [35] Y.X. Yao, X. Chen, C. Yan, et al., *Angew. Chem. Int. Ed.* 60 (2020) 4090–4097.
- [36] T.D. Pham, K.K. Lee, *Small* 17 (2021) 2100133.
- [37] K. Ding, C. Xu, Z. Peng, et al., *ACS Appl. Mater. Interfaces* 14 (2022) 44470–44478.
- [38] J. Zhang, Q. Li, Y. Zeng, et al., *ACS Energy Lett.* 8 (2023) 1752–1761.
- [39] Z. Li, Y. Chen, X. Yun, et al., *Adv. Funct. Mater.* 33 (2023) 2300502.
- [40] Z. Yu, P.E. Rudnicki, Z. Zhang, et al., *Nat. Energy* 7 (2022) 94–106.
- [41] A. Wang, Y. Song, Z. Zhao, et al., *Adv. Funct. Mater.* 33 (2023) 2302503.
- [42] Q. Sun, Z. Cao, Z. Ma, et al., *ACS Energy Lett.* 7 (2022) 3545–3556.
- [43] Y. Wang, Z. Cao, Z. Ma, et al., *ACS Energy Lett.* 8 (2023) 1477–1484.
- [44] Y. Zou, Z. Ma, G. Liu, et al., *Angew. Chem. Int. Ed.* 62 (2023) e202216189.
- [45] M.R. Chanan, D. Sessler, Sabine Becker, et al., *J. Am. Chem. Soc.* 139 (2017) 9325–9332.
- [46] Y. Zafrani, D. Yeffet, G. Sod-Moriah, et al., *J. Med. Chem.* 60 (2017) 797–804.
- [47] S. Liu, X. Ji, N. Piao, et al., *Angew. Chem. Int. Ed.* 60 (2020) 3661–3671.
- [48] G. Zhang, J. Li, S.S. Chi, et al., *Adv. Funct. Mater.* 33 (2023) 2312413.